

Delay Approximations for Correlation Measurements Using Analog Computers

GUILLERMO GONZÁLEZ

Abstract—In the most direct method for measuring correlation functions with an analog computer a delay must be simulated. Since a lumped parameter system is used, we can only hope to approximate this delay. We intentionally exclude such storage systems as magnetic tapes because of their cost, and confine ourselves to the use of commonly available analog computer components.

Extensive work has been carried out toward finding the best delay approximation according to different criteria, based mainly on transient or frequency response considerations. In this paper a new point of view is adopted. The overall effect of the delay approximation on the measured value of the autocorrelation function is taken into account. The best approximation is then chosen as the one that produces the closest agreement between the theoretically measured value and the exact value of the autocorrelation. It is seen that this method for selecting the delay approximation sometimes leads to very different results from those formerly obtained. For example, it is shown that for measuring the autocorrelation of noise generated by filtering white noise with a filter with real poles, the best approximation is one whose value for a real argument (instead of $j\omega$) best approaches the exponential function for a real argument.

The treatment of the subject in this paper deals mainly with the autocorrelation function, but is later extended to the case of cross-correlations.

GENERAL EQUATION

LET $\{x(t)\}$ be an ergodic random process with an auto-variance $K_x(\tau)$ and a corresponding power spectral density $W_x(\omega)$. Since the process is ergodic, the autocorrelation measured for one of the members $x(t)$ of the process is equal to the auto-variance of the process. Therefore [1],

$$K_x(\tau) = R_x(\tau)$$

and

$$K_x(\tau) = \lim_{T \rightarrow \infty} \frac{1}{T} \int_{-T/2}^{T/2} x(t)x(t + \tau)dt. \quad (1)$$

But since we are dealing with a physical measurement starting at $t=0$, we must use

$$R_x(\tau) = \lim_{T \rightarrow \infty} \frac{1}{T} \int_0^T x(t)x(t - \tau)dt. \quad (2)$$

However, (2) gives the same result as (1) if the process is ergodic [1]. The measurement is subject to a restriction concerning the integration time T which, of course, must be finite. This part of the problem is treated elsewhere in the literature [1].

Ideally, the circuit for obtaining $R_x(\tau)$ would be the one shown in Fig. 1. It appears that if we could use a

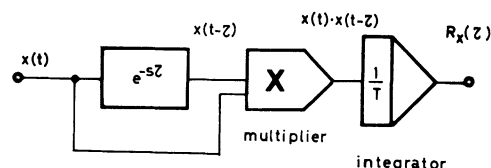


Fig. 1. Ideal circuit for measuring $R_x(\tau)$.

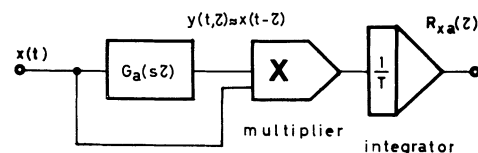


Fig. 2. Circuit for measuring $R_{xa}(\tau) \approx R_x(\tau)$.

system with a transfer function $G_a(s\tau) = e^{-s\tau}$, we would be able to obtain $R_x(\tau)$ with any accuracy we might prescribe, if the integration time were long enough.

Since $e^{-s\tau}$ cannot be synthesized by means of lumped parameter systems, such as we have in an electronic analog computer, a rational fraction approximation to the complex exponential function must be found. Extensive work has been carried out along these lines according to different approximating criteria [2]–[4]. Our new criterion will be that of finding the best delay approximation, considering its overall effect on the measurement of the autocorrelation function itself.

If we use any of the approximations $G_a(s\tau)$ in place of the delay $e^{-s\tau}$, we shall have the system of Fig. 2 for carrying out our measurement. Let us find what is really measured, instead of $R_x(\tau)$, because of that imperfect delay realization. Let

$R_{xa}(\tau)$ = approximation of $R_x(\tau)$ measured by the system of Fig. 2;

$G_a(s\tau)$ = approximation of $e^{-s\tau}$ used in this system;

$y(t, \tau)$ = approximation of $x(t - \tau)$.

In the measurement of $R_{xa}(\tau)$, for a certain value of τ the value of τ is fixed in $G_a(s\tau)$, and the time average of $x(t)y(t, \tau)$ is found by a multiplication followed by an integration, i.e.,

$$R_{xa}(\tau) = \lim_{T \rightarrow \infty} \frac{1}{T} \int_0^T x(t)y(t, \tau)dt. \quad (3)$$

Let us now relate $R_{xa}(\tau)$ to the crosscorrelation between $x(t)$ and $y(t, \tau)$. For a fixed τ we have at the inputs of the multiplier two signals which are functions of time: $x(t)$ and $y(t, \tau)$. If we now take τ_1 as the new delay parameter, the crosscorrelation between these signals is

$$R_{yx}(-\tau_1) = \lim_{T \rightarrow \infty} \frac{1}{T} \int_0^T x(t - \tau_1)y(t, \tau)dt. \quad (4)$$

We note that τ in (4) is just a fixed parameter and not the delay parameter. If we set here $\tau_1=0$, we get

$$R_{yx}(0) = \lim_{T \rightarrow \infty} \frac{1}{T} \int_0^T x(t)y(t, \tau)dt, \quad (5)$$

and, comparing with (3),

$$R_{za}(\tau) = R_{yx}(0). \quad (6)$$

That is, for the crosscorrelation parameter equal to zero, the approximation $R_{za}(\tau)$ of $R_x(\tau)$ is the crosscorrelation between $x(t)$ and the approximation $y(t, \tau)$ of the delayed input $x(t-\tau)$.

For the system of Fig. 3 we may write [1]

$$W_{yz}(\omega) = G_1(j\omega)G_2^*(j\omega)W_x(\omega). \quad (7)$$

Here $W_{yz}(\omega)$ is the cross power spectral density related to the signals $y(t)$ and $z(t)$. In our case (Fig. 2) we may set

$$\begin{aligned} G_2(j\omega) &= 1 = G_2^*(j\omega), \\ z(t) &= x(t), \\ G_1(s\tau) &= G_a(s\tau), \\ G_1(j\omega\tau) &= G_a(j\omega\tau). \end{aligned}$$

Replacing these relations in (7) we obtain

$$\begin{aligned} W_{yz}(\omega) &= W_{yx}(\omega), \\ W_{yz}(\omega) &= G_a(j\omega\tau)W_x(\omega). \end{aligned} \quad (8)$$

Now, according to the Wiener-Khinchine theorem [1],

$$\begin{aligned} K_{yx}(v) &= \frac{1}{2} F W_{yx}(\omega), \\ K_{yx}(v) &= \frac{1}{2} \int_{-\infty}^{\infty} e^{j\omega v} W_{yx}(\omega) \frac{d\omega}{2\pi}. \end{aligned} \quad (9)$$

But because of our ergodic hypothesis,

$$K_{yx}(v) = R_{yx}(v). \quad (10)$$

Then, from (8), (9), and (10) we may write

$$\begin{aligned} R_{yx}(v) &= \frac{1}{2} \int_{-\infty}^{\infty} e^{j\omega v} G_a(j\omega\tau) W_x(\omega) \frac{d\omega}{2\pi} \\ R_{yx}(0) &= \frac{1}{2} \int_{-\infty}^{\infty} G_a(j\omega\tau) W_x(\omega) \frac{d\omega}{2\pi}. \end{aligned}$$

Finally, using (6), the general equation (11) is obtained, giving the approximate autocorrelation function as a function of the delay approximation transfer function and the noise power density spectrum:

$$R_{za}(\tau) = \frac{1}{2} \int_{-\infty}^{\infty} G_a(j\omega\tau) W_x(\omega) \frac{d\omega}{2\pi}. \quad (11)$$

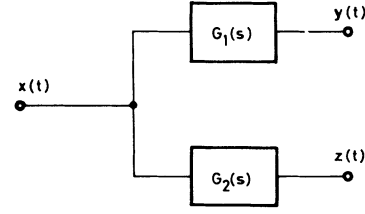


Fig. 3. $W_{yz}(\omega) = G_1(j\omega)G_2^*(j\omega)W_x(\omega)$.

As will be shown, this equation sets the basis for the determination of the best approximation $G_a(j\omega\tau)$. In the ideal case,

$$G_a(j\omega\tau) = e^{-j\omega\tau},$$

and (11) agrees with the Wiener-Khinchine theorem for $\tau \geq 0$. In effect, we now have

$$R_x(\tau) = R_{za}(\tau) = \frac{1}{2} \int_{-\infty}^{\infty} e^{j\omega\tau} W_x(\omega) \frac{d\omega}{2\pi}.$$

Instead of adopting the best approximation $G_a(j\omega\tau)$ as that which more closely approximates $e^{-j\omega\tau}$, we shall select that $G_a(j\omega\tau)$ which produces the best approximation of $R_{za}(\tau)$ to $R_x(\tau)$. This last method often leads to quite different results for $G_a(j\omega\tau)$ when compared with results formerly obtained.

Equation (11) may be put in a form more suitable for calculation, noting that it is the evaluation along the $j\omega$ axis of the integral

$$\frac{1}{4\pi j} \int G_a(s\tau) W_x\left(\frac{s}{j}\right) ds.$$

Hence,

$$R_{za}(\tau) = \frac{1}{4\pi j} \int_{-j\infty}^{j\infty} G_a(s\tau) W_x\left(\frac{s}{j}\right) ds. \quad (12)$$

In many cases (12) may be evaluated in a relatively easy way by using Cauchy's residue theorem [5]:

$$\begin{aligned} \oint_C f(s) ds \\ = 2\pi j \sum \text{Res} [f(s), \text{at poles of } f(s) \text{ inside } C]. \end{aligned} \quad (13)$$

Let $f(s)$ in (13) be

$$f(s) = G_a(s\tau) W_x\left(\frac{s}{j}\right). \quad (13a)$$

Then, with reference to Fig. 4, we write

$$\begin{aligned} \oint_C f(s) ds &= \int_{+jR}^{-jR} f(s) ds + \oint_{C_2} f(s) ds \\ &= 2\pi j \sum \text{Res} [f(s), \text{in } C_1 + C_2]. \end{aligned} \quad (14)$$

Because $G_a(s\tau)$ is a stable function, it has no poles in the right-half plane (RHP). The only poles inside $C_1 + C_2$ are then those of $W_x(s/j)$, with the exception of the poles of $W_x(s/j)$ at the origin, which must be left

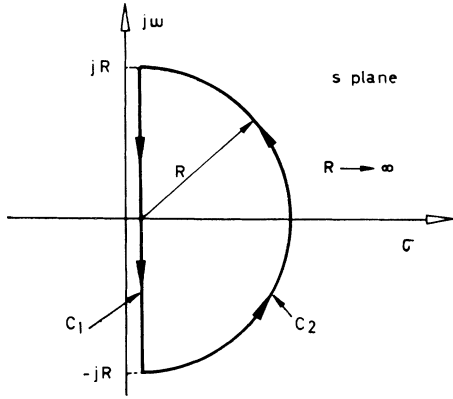


Fig. 4. Integration contour for integral (13).

out of the integration contour. Accordingly, letting R go to infinity, (14) gives the following equation:

$$\begin{aligned}
 & - \int_{-j\infty}^{j\infty} f(s) ds \\
 & = 2\pi j \sum \text{Res} \left[G_a(s\tau) W_x \left(\frac{s}{j} \right) \text{ at poles of } W \left(\frac{s}{j} \right) \text{ in } RHP \right] \\
 & + \lim_{R \rightarrow \infty} \oint_{C_2} f(s) ds.
 \end{aligned}$$

In many cases we find that

$$\lim_{R \rightarrow \infty} \oint_{C_2} f(s) ds = 0. \quad (\text{See Appendix.}) \quad (15)$$

Therefore,

$$\begin{aligned}
 & \int_{-j\infty}^{j\infty} G_a(s\tau) W_x \left(\frac{s}{j} \right) ds \\
 & = - 2\pi j \sum \text{Res} \left[G_a(s\tau) W_x \left(\frac{s}{j} \right) \text{ at } P_{WRP} \right].
 \end{aligned}$$

Here P_{WRP} are the poles of $W_x(s/j)$ in the right-half plane. Finally, replacing this expression in (12), the approximation $R_{xa}(\tau)$ of $R_x(\tau)$ is found to be

$$R_{xa}(\tau) = - \frac{1}{2} \sum \text{Res} \left[G_a(s\tau) W_x \left(\frac{s}{j} \right) \text{ at } P_{WRP} \right], \quad (16)$$

subject to the restriction imposed by (15).

APPLICATION TO RATIONAL SPECTRUM NOISE

The output power spectral density $W_x(\omega)$ of a linear lumped parameter system with a transfer function $H(j\omega)$ is related [1], [6] to its input power spectral density $W_i(\omega)$ by

$$W_x(\omega) = |H(j\omega)|^2 W_i(\omega).$$

If the input signal is white noise with $W_i(\omega) = W_0$, the output is rational spectrum noise, and is given by

$$W_x(\omega) = |H(j\omega)|^2 W_0 = W_0 H(j\omega) H(-j\omega). \quad (17)$$

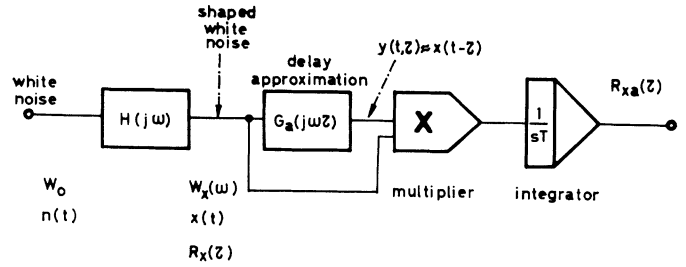


Fig. 5. Measurement of the autocorrelation approximation of linearly filtered white noise.

According to (16), the approximation given by the correlation circuit of Fig. 5 is

$$\begin{aligned}
 R_{xa}(\tau) & = - \frac{1}{2} \sum \text{Res} [G_a(s\tau) H(s) H(-s) W_0, \text{ at } P_{WRP}], \quad (18)
 \end{aligned}$$

where P_{WRP} are the poles of $H(s) H(-s)$ in the right-half plane.

If we assume that the filter $H(s)$ is a stable system, the poles of $H(s)$ are all in the left-half plane. Consequently, the poles of $H(-s)$ are all in the right-half plane. Hence, the poles of $H(s) H(-s)$ in the RHP are those of $H(-s)$. Therefore,

$$R_{xa}(\tau) = - \frac{W_0}{2} \sum \text{Res} [G_a(s\tau) H(s) H(-s) \text{ at } P_{HRP}], \quad (19)$$

where P_{HRP} are the poles of $H(-s)$ in the right-half plane. Let

$$\begin{aligned}
 H(s) & = K \frac{(s + z_1)(s + z_2) \cdots (s + z_m)}{(s + p_1)(s + p_2) \cdots (s + p_n)} \\
 & = \frac{Q_m(s)}{P_n(s)} \quad m < n,
 \end{aligned}$$

with the simple poles $-p_i$, real or complex, in the left-half plane. Then,

$$H(s) H(-s) = K^2 \frac{Q_m(s) Q_m(-s)}{(s + p_1)(s - p_1) \cdots (s + p_n)(s - p_n)}.$$

In order to use (19) we must find

$$\begin{aligned}
 & \text{Res} [G_a(s\tau) H(s) H(-s), p_i] \\
 & = \lim_{s \rightarrow p_i} (s - p_i) G_a(s\tau) H(s) H(-s),
 \end{aligned}$$

since p_i are the poles of $H(-s)$. Noting that $G_a(s\tau)$ has no poles in the RHP , we may write

$$\begin{aligned}
 & \text{Res} [G_a(s\tau) H(s) H(-s), p_i] \\
 & = G_a(p_i\tau) \lim_{s \rightarrow p_i} (s - p_i) H(s) H(-s). \quad (20)
 \end{aligned}$$

But if we let

$$A_{-i} = \lim_{s \rightarrow p_i} (s - p_i) H(s) H(-s),$$

we may write the following:

$$A_{-i} = \lim_{-s \rightarrow -p_i} (-s - p_i)H(-s)H(s).$$

Hence,

$$A_{-i} = \lim_{s \rightarrow -p_i} (s + p_i)H(s)H(-s) = -A_i.$$

Then

$$A_i = - \lim_{s \rightarrow -p_i} (s + p_i)H(s)H(-s), \tag{21}$$

replaced in (20), yields

$$\text{Res} [G_a(s\tau)H(s)H(-s), p_i] = -A_i G_a(p_i\tau).$$

Finally, replacing this in (19), the approximation to the autocorrelation function is found to be

$$R_{xa}(\tau) = \frac{W_0}{2} \sum_{i=1}^n A_i G_a(p_i\tau), \quad \tau \geq 0 \tag{22}$$

where W_0 is the power density spectrum of the white noise at the input of $H(s)$ (see Fig. 5); $-p_i$ are the poles of $H(s)$ (all poles are simple and in the left-hand plane); A_i is the residue of $H(s)H(-s)$ at $-p_i$ ($i=1 \dots n$); and $G_a(s\tau)$ is the delay approximation transfer function.

If $H(s)$ has a pole of order r at $-p_j$, the residue is

$$A_{-j,r} = \text{Res} [G_a(s)H(s)H(-s), p_j],$$

$$A_{-j,r} = \lim_{s \rightarrow p_j} \frac{1}{(r-1)!} \frac{d^{r-1}}{ds^{r-1}} [(s - p_j)^r G_a(s)H(s)H(-s)],$$

and (22) turns into a more complicated expression. It is simpler in this case to treat the problem as a particular situation starting from (19), rather than try to find a more elaborate formula in place of (22).

If in (22) we let

$$G_a(s\tau) = e^{-s\tau},$$

the exact autocorrelation function is obtained for $\tau \geq 0$:

$$R_{xa}(\tau) = R_x(\tau) = \frac{W_0}{2} \sum_{i=1}^n A_i e^{-p_i\tau}, \quad \tau \geq 0. \tag{23}$$

Since the function measured by the circuit of Fig. 5 is the approximation

$$R_{za}(\tau) = \sum_{i=1}^n A_i G_a(p_i\tau), \tag{24}$$

and since its exact value is given by

$$R_x(\tau) = \sum_{i=1}^n A_i e^{-p_i\tau},$$

the error is

$$E(\tau) = R_x(\tau) - R_{za}(\tau),$$

that is,

$$E(\tau) = \sum_{i=1}^n A_i [e^{-p_i\tau} - G_a(p_i\tau)]. \tag{25}$$

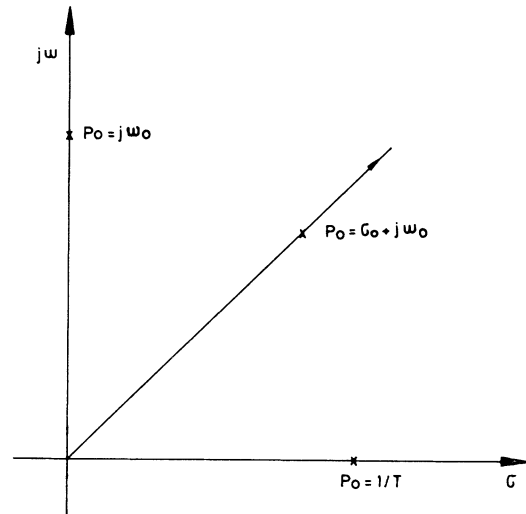


Fig. 6. Domain for the valuation of the complex frequency response.

Let

$$E_i(\tau) = e^{-p_i\tau} - G_a(p_i\tau), \tag{26}$$

so that

$$E(\tau) = \sum_{i=1}^n A_i E_i(\tau). \tag{27}$$

Then the accuracy of the measurement shall depend on the differences

$$e^{-p_i\tau} - G_a(p_i\tau),$$

within the range of τ concerned. This means that we must study $G(p_i\tau)$, as τ varies, and compare it with $e^{-p_i\tau}$. To do this, it is convenient to use the concept of a complex frequency response, defined as the set of values a function $G(\lambda p_0)$ assumes as λ varies.

Here p_0 is, in general, a fixed complex number, while λ is real and variable. This corresponds to the evaluation of $G(\lambda p_0)$ along an axis passing through $0 + j0$, for $\lambda = 0$, and through p_0 , for $\lambda = 1$. For $p_0 = j$ and $\lambda = \omega$ we obtain the special case of the frequency response. For $p_0 = 1/T$, real, we have the evaluation of $G(\lambda p_0)$ along the real axis. These situations are shown in Fig. 6.

Let us study the complex frequency response of $G_a(p_i\tau)$ in (24) and (26) according to the different nature of the poles p_i .

Real Poles

Let $p_i = 1/T_i$ be real. Then,

$$G_a(p_i\tau) = G_a\left(\frac{\tau}{T_i}\right),$$

and

$$E_i(\tau) = e^{-(\tau/T_i)} - G_a\left(\frac{\tau}{T_i}\right).$$

We see, then, that for a real pole of $H(s)$ in Fig. 5, the best $G_a(s\tau)$ will be the one whose real axis response

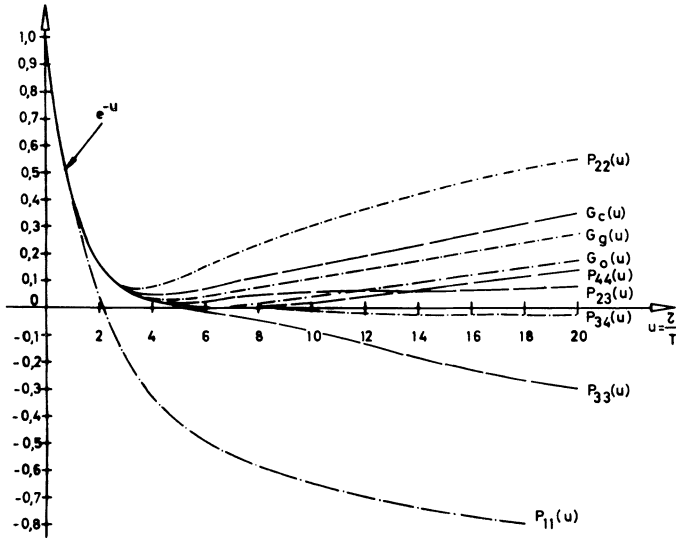


Fig. 7. Value of the approximations for a real argument.

$G(\tau/T_i)$ best approximates the exponential for a real argument, i.e., $e^{-(\tau/T)}$, within the range of τ/T of interest. Since the nondimensional variable τ/T is independent of any particular real pole, we immediately conclude that, if all the poles of $H(s)$ are real, then the best delay approximation is also that which best approximates $e^{-(\tau/T)}$.

In Fig. 7 we find $G_a(u) = G_a(\tau/T)$ for some rational fraction approximations of $G(s\tau)$ which can be built with commonly available analog computer components.

These are described in the literature [2], [4], [7] and have the following transfer functions:

1) Graphically determined optimum (in frequency domain) fourth-order all-pass approximation:

$$G_g(s\tau) = \frac{1073.8 - 536.9(s\tau) + 119.96(s\tau)^2 - 13.585(s\tau)^3 + (s\tau)^4}{1073.8 + 536.9(s\tau) + 119.96(s\tau)^2 + 13.585(s\tau)^3 + (s\tau)^4} \tag{28}$$

2) All derivatives of the phase response equal to zero at $s\tau = j\omega\tau = 0$:

$$G_0(s\tau) = \frac{1415.9 - 715.73(s\tau) + 155.85(s\tau)^2 - 180576(\tau s)^3 + (\tau s)^4}{1415.9 + 715.73(s\tau) + 155.85(s\tau)^2 + 180576(\tau s)^3 + (\tau s)^4} \tag{29}$$

3) Cut product approximation:

$$G_c(s\tau) = \frac{876.68 - 438.34(s\tau) + 98.696(s\tau)^2 - 11.10(\tau s)^3 + (\tau s)^4}{876.68 + 438.34(s\tau) + 98.696(s\tau)^2 + 11.10(s\tau)^3 + (s\tau)^4} \tag{30}$$

The Padé approximations plotted in Fig. 7 are

$$P_{11}(s\tau) = \frac{2 - s\tau}{2 + s\tau} \tag{31}$$

$$P_{22}(s\tau) = \frac{12 - 6(s\tau) + (s\tau)^2}{12 + 6(s\tau) + (s\tau)^2} \tag{32}$$

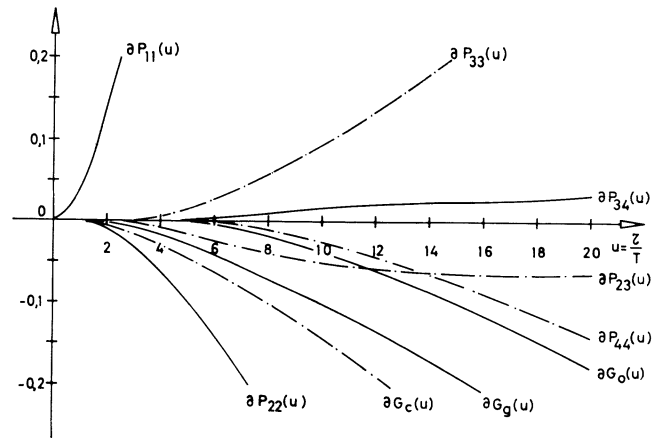


Fig. 8. Error $E(\tau) = \delta G_a(\tau) = e^{-u} - G_a(u)$ for different approximations and a real argument.

$$P_{23}(s\tau) = \frac{60 - 24(s\tau) + 3(s\tau)^2}{60 + 36(s\tau) + 9(s\tau)^2 + (s\tau)^3} \tag{33}$$

$$P_{33}(s\tau) = \frac{120 - 60s\tau + 12(s\tau)^2 - (s\tau)^3}{120 + 60s\tau + 12(s\tau)^2 + (s\tau)^3} \tag{34}$$

$$P_{34}(s\tau) = \frac{840 - 360(s\tau) + 60(s\tau)^2 - 4(s\tau)^3}{840 + 480(s\tau) + 120(s\tau)^2 + 16(s\tau)^3 + (s\tau)^4} \tag{35}$$

$$P_{44}(s\tau) = \frac{1680 - 840(s\tau) + 180(s\tau)^2 - 20(s\tau)^3 + (s\tau)^4}{1680 + 840(s\tau) + 180(s\tau)^2 + 20(s\tau)^3 + (s\tau)^4} \tag{36}$$

In Fig. 8 we find plots of the error

$$E(\tau) = e^{-(\tau/T)} - G_a\left(\frac{\tau}{T}\right) = \delta G_a\left(\frac{\tau}{T}\right).$$

As is to be expected, the error introduced by all-pass approximations begins to increase after a certain τ/T ,

since as τ/T goes to infinity, $G_a(\tau/T)$ must reach plus or minus one. However, the non-all-pass approximations,

such as $P_{23}(\tau/T)$ and $P_{34}(\tau/T)$, go to zero under these

same circumstances. Since $e^{-(\tau/T)}$ goes to zero as τ/T tends to infinity, they are better suited for representing $e^{-(\tau/T)}$.

For example, let $H(s)$ in Fig. 5 be

$$H(s) = \frac{1}{sT_0 + 1}$$

Then, from (21),

$$A_i = \lim_{s \rightarrow -1/T_0} \frac{1}{sT_0 + 1} \frac{1}{1 - sT_0} \left(s + \frac{1}{T_0} \right),$$

$$A_i = 1/2T_0,$$

and, from (22),

$$R_{xa}(\tau) = \frac{W_0}{4T_0} G_a \left(\frac{\tau}{T_0} \right).$$

The exact value is given by

$$R_x(\tau) = \frac{W_0}{4T_0} e^{-(\tau/T_0)}, \quad \tau \geq 0.$$

Since

$$R_x(0) = R_{xa}(0) = \frac{W_0}{4T_0},$$

we may write the normalized autocorrelation

$$r_{xa}(\tau) = \frac{R_{xa}(\tau)}{R_x(0)} = G_a \left(\frac{\tau}{T_0} \right).$$

We observe from Fig. 8 that if we use $P_{34}(s\tau)$ as the delay approximation for the measurement, we get an error of 1.5 per cent, for $\tau/T = 10$. If $G_g(s\tau)$ is used, the error goes up to 10 per cent. $P_{23}(s\tau)$ would produce an error of 5 per cent under these same circumstances.

As another illustrative example let us choose

$$H(s) = \frac{1}{(1 + sT_1)(1 + sT_2)}.$$

Then,

$$A_1 = \lim_{s \rightarrow -1/T_1} \left(s + \frac{1}{T_1} \right) H(s)H(-s) = \frac{T_1}{2(T_1^2 - T_2^2)},$$

and

$$A_2 = \lim_{s \rightarrow -1/T_2} \left(s + \frac{1}{T_2} \right) H(s)H(-s) = -\frac{T_2}{T_1} A_1.$$

Hence, from (22),

$$R_{xa}(\tau) = \frac{W_0}{2} \left[A_1 G_a \left(\frac{\tau}{T_1} \right) + A_2 G_a \left(\frac{\tau}{T_2} \right) \right],$$

$$R_{xa}(\tau) = \frac{1}{2} A_1 W_0 \left[G_a \left(\frac{\tau}{T_1} \right) - \frac{T_2}{T_1} G_a \left(\frac{\tau}{T_2} \right) \right].$$

Also,

$$r_{xa}(\tau) = \frac{R_{xa}(\tau)}{R_{xa}(0)},$$

so that

$$r_{xa}(\tau) = \frac{T_1}{T_1 - T_2} \left[G_a \left(\frac{\tau}{T_1} \right) - \frac{T_2}{T_1} G_a \left(\frac{\tau}{T_2} \right) \right]. \quad (37)$$

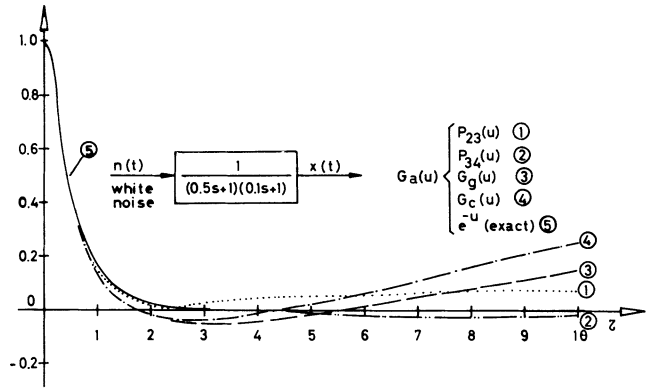


Fig. 9. Calculated $r_{xa}(\tau)$ for different approximations and filtered white noise.

We see that even if τ/T_1 is not very large (i.e., the errors caused by all-pass approximations are not high), it may happen that $\tau/T_2 = T_1/T_2(\tau/T_1)$ is large, giving rise to a significant error in $G_a(\tau/T_2)$. However, this effect is partially reduced because of the factor T_2/T_1 in

$$\frac{T_2}{T_1} G_a \left(\frac{\tau}{T_2} \right).$$

For example, let

$$T_1 = 0.5,$$

$$T_2 = 0.1.$$

From (37) we have

$$r_{xa}(\tau) = 1.25[G_a(2\tau) - 0.2G_a(10\tau)],$$

which is plotted in Fig. 9 for various delay approximations.

For $\tau = 1$, we have $G_a(2)$ in the first term, but $G_a(10)$ in the second. It is here that an all-pass approximation is undesirable because of its higher error for large arguments.

In Fig. 9 we see that, up to $\tau = 10$, the maximum error introduced by using $P_{34}(s\tau)$ is less than 4 per cent, while if $G_g(s\tau)$ is used, this error rises to 15 per cent. Even $P_{23}(s\tau)$ is better for this case, since the error reaches only 7 per cent.

As a final example of $H(s)$ with real poles, let

$$H(s) = \frac{sT_0}{(sT_0 + 1)(sT_1 + 1)(sT_2 + 1)}.$$

This form appears when a filter for dc suppression, with a transfer function $sT_0/sT_0 + 1$, is used in cascade with two low-pass filters.

Following the procedure already outlined, we obtain from (21) and (22)

$$A_0 = \frac{T_0^3}{2(T_0^2 - T_1^2)(T_0^2 - T_2^2)},$$

$$A_1 = \frac{T_0^2 T_1}{2(T_0^2 - T_1^2)(T_1^2 - T_2^2)},$$

$$A_2 = \frac{T_0^2 T_2}{2(T_0^2 - T_2^2)(T_1^2 - T_2^2)},$$

and

$$r_{xa}(\tau) = \frac{A_0 G_a\left(\frac{\tau}{T_0}\right) + A_1 G_a\left(\frac{\tau}{T_1}\right) + A_2 G_a\left(\frac{\tau}{T_2}\right)}{A_0 + A_1 + A_2}. \quad (38)$$

If we let

$$T_0 = 10$$

$$T_1 = 0.5$$

$$T_2 = 0.2,$$

replacing in (38) we find

$$r_{xa}(\tau) = 1.493[-0.05G_a(0.1\tau) + 1.193G_a(2\tau) - 0.476G_a(5\tau)].$$

This function is plotted in Fig. 10. Again we see that by the use of $P_{23}(s\tau)$ and $P_{34}(s\tau)$ as delay approximations, better results are obtained than if all-pass approximations were used.

Complex Poles

Let p_i in

$$R_{xa}(\tau) = \frac{W_0}{2} \sum_{i=1}^n A_i G_a(p_i \tau) \quad (39)$$

be complex. Then we may write

$$p_i = \sigma_i + j\omega_i,$$

$$p_i = \xi_i \omega_{ni} + j\omega_{ni} \sqrt{1 - \xi_i^2},$$

$$p_i \tau = \omega_{ni} \tau (\xi_i + j\sqrt{1 - \xi_i^2}),$$

where ω_{ni} is the natural frequency of the pole and ξ_i its damping factor. Then,

$$G_a(p_i \tau) = G_a[\omega_{ni} \tau (\xi_i + j\sqrt{1 - \xi_i^2})]. \quad (40)$$

In order to compare with the case of real poles, let us write $\omega_{ni} = 1/T_{ni}$. We obtain

$$G_a(p_i \tau) = G_a\left[\frac{\tau}{T_{ni}} (\xi_i + j\sqrt{1 - \xi_i^2})\right].$$

The argument here is not independent of the different poles $-p_i$ of $H(s)$ because of ξ_i . Instead of having only one function $G_a(\tau/T)$, as in the case of real poles, we have a family of functions of the nondimensional variable $\omega_n \tau = \tau/T_n$, with ξ as a parameter.

The complex frequency response of $G_a(p\tau)$ may be seen in Fig. 11 for different delay approximations, and for the perfect delay

$$e^{-p\tau} = e^{-\xi(\omega_n \tau)} e^{+j(\omega_n \tau)} \sqrt{1 - \xi^2}.$$

As in the case of real poles, the error appears for the larger values of τ/T_n or $\omega_n \tau$. The complex frequency response of $e^{-p\tau}$ is such that its amplitude goes to zero as $\omega_n \tau$ increases, for $\xi > 0$. This happens more rapidly the higher ξ may be, while if $\xi = 0$, $e^{-p\tau}$ does not go to

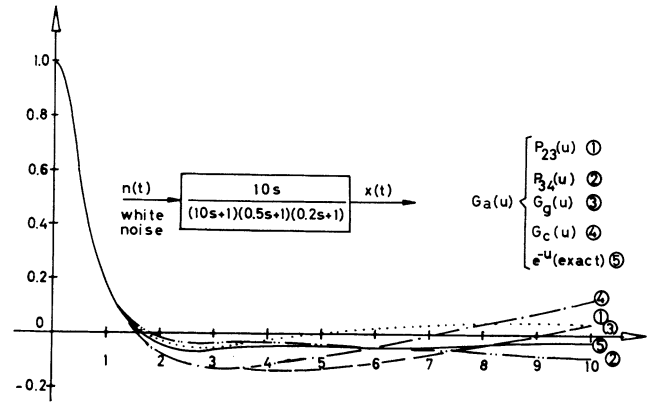


Fig. 10. Approximation $r_{xa}(\tau)$ of filtered white noise for different delay approximations.

zero at all. This is why we observe in Fig. 11 that for the higher values of ξ , non-all-pass approximations are better than the all-pass ones, while for the lower range of ξ the converse is true. We see this confirmed by the results of Example 1.

Example 1: Let white noise be the input to a second-order system with a transfer function

$$H(s) = \frac{\omega_n^2}{s^2 + 2\xi\omega_n s + \omega_n^2}. \quad (41)$$

The approximate autocorrelation that would be measured at its output, for different delay approximations (Fig. 5), may be calculated by use of (22). The results are plotted in Figs. 12(a), (b), (c), (d), and (e) for $\xi = 0.1, 0.3, 0.5, 0.7,$ and 0.9 , respectively.

Among the many error criteria that may be considered for comparing the relative merits of the different approximations, let us choose one that will give the maximum $\omega_n \tau$ for which the difference between the actual and the measured value of the autocorrelation is less than ϵ ; let us call this value $\omega_n \tau_m$. Choosing $\epsilon = 0.02$ and 0.05 , we may construct Tables I and II with the aid of Fig. 12.

Example 2: Suppose we are required to select a delay approximation for measuring the autocorrelation function $r_x(\tau)$ of white noise filtered by a second-order system in which ξ may be between 0.9 and 0.5 . The normalized value shall be within 0.02 of the actual value. This measurement is to be carried out up to $\omega_n \tau = 4.0$ in one case, and up to $\omega_n \tau = 6.5$ in the other. In Table I we see that for the first case we may use $P_{34}(s\tau)$, $G_0(s\tau)$, or $G_g(s\tau)$; for the second case we may use only $P_{34}(s\tau)$.

Example 3: Let us change the range of ξ in Example 2, and suppose that it is between 0.1 and 0.5 , and that the measurement is to be carried out up to $\omega_n \tau = 4.5$, and $\omega_n \tau = 5.5$. Now in Table I we find that for both of these cases we may use either $G_0(s\tau)$ or $G_g(s\tau)$.

Sinusoidal Signal

The autocorrelation of a sinusoidal signal

$$x(t) = A_0 \cos(\omega_0 t + \phi),$$

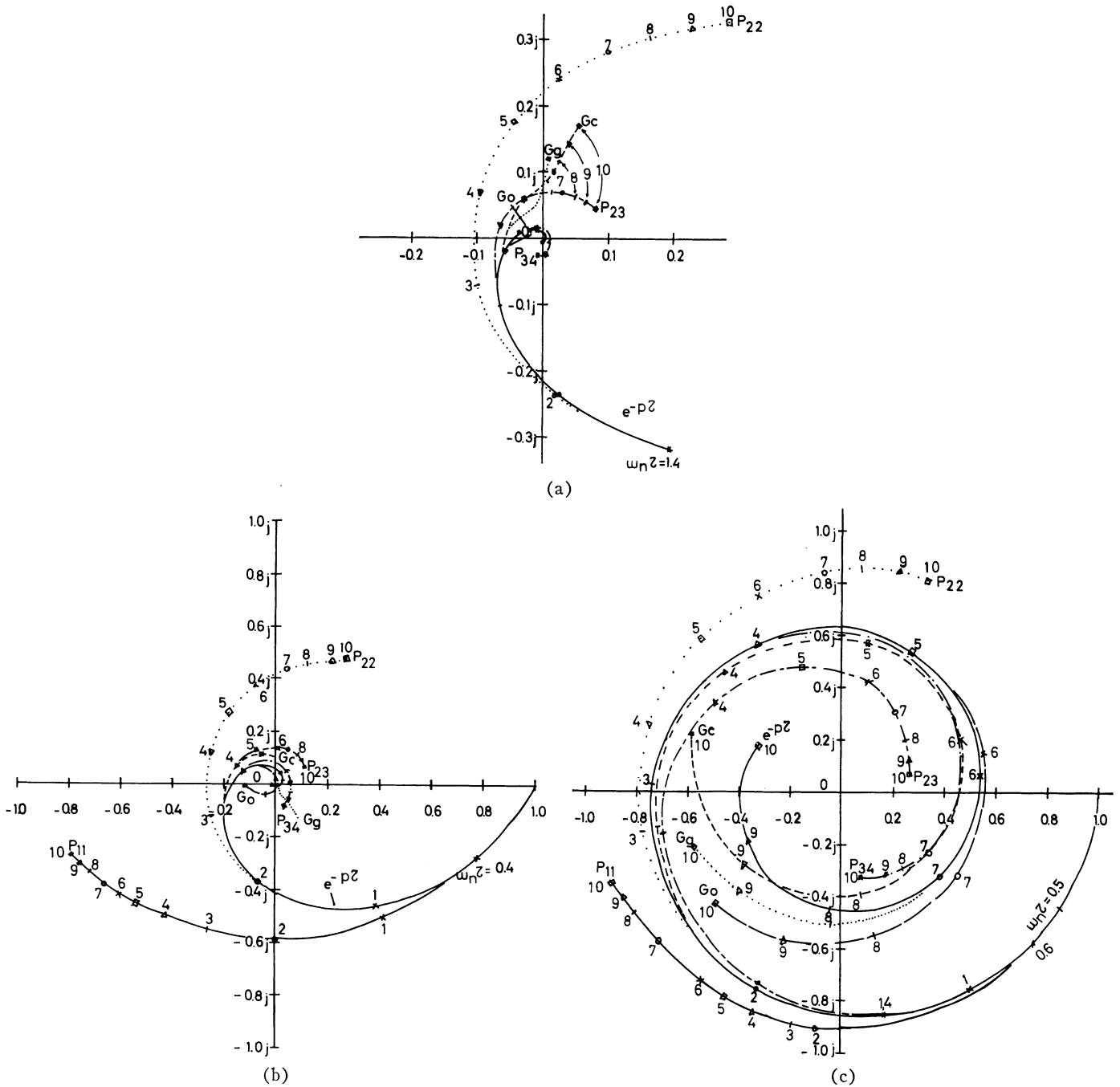


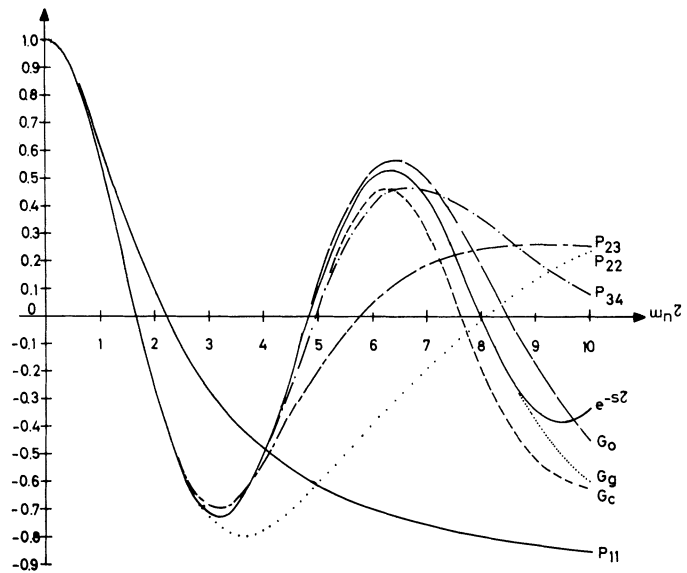
Fig. 11. Complex frequency response of several approximations $G_a(p\tau)$ for complex pole pairs: (a) $\xi=0.7$; (b) $\xi=0.5$; and (c) $\xi=0.1$. The parameter shown in the curves is $\omega_n\tau$.

TABLE I

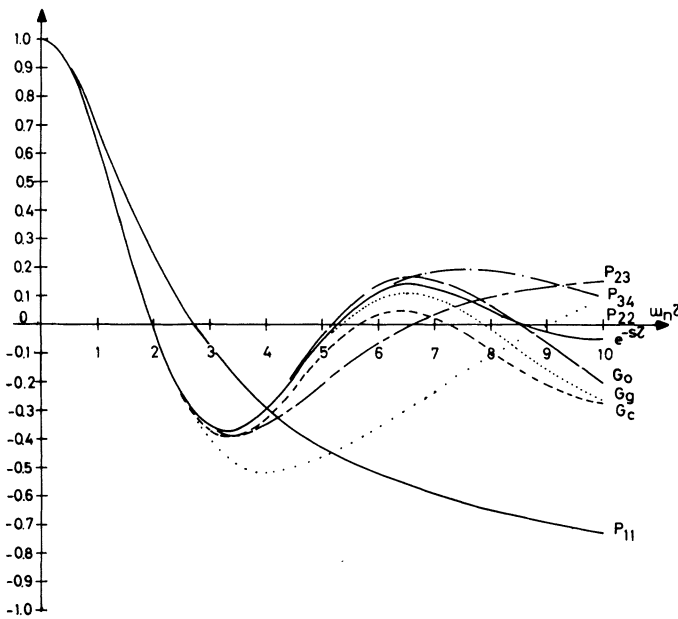
Approximate values of $\omega_n\tau_m$ such that $ r_x(\tau) - r_{xa}(\tau) < 0.02$ for $\omega_n\tau < \omega_n\tau_m$.				
$G_a(s\tau)$	$P_{23}(s\tau)$	$P_{34}(s\tau)$	$G_0(s\tau)$	$G_g(s\tau)$
real pole	5.2	> 10	8.4	4.4
$\xi=0.9$	> 10	> 10	5.9	4.5
0.7	3.3	6.5	6.6	4.5
0.5	3.3	6.5	7.8	5.6
0.3	3.5	6.5	5.5	6.1
0.1	2.6	4.0	6.2	8.9

TABLE II

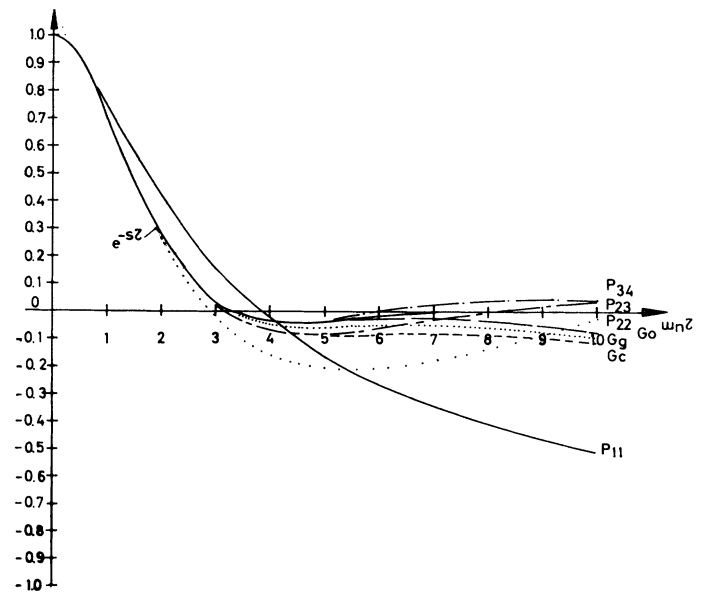
$\omega_n\tau_m$ for $\xi=0.05$.				
$G_a(s\tau)$	$P_{23}(s\tau)$	$P_{34}(s\tau)$	$G_0(s\tau)$	$G_g(s\tau)$
real pole	9.6	> 20	> 10	6.8
$\xi=0.9$	> 10	> 10	8.5	5.8
0.7	> 10	> 10	8.6	7.0
0.5	4.2	7.4	7.8	7.1
0.3	4.0	6.7	9.1	7.8
0.1	4.1	5.0	6.8	9.2



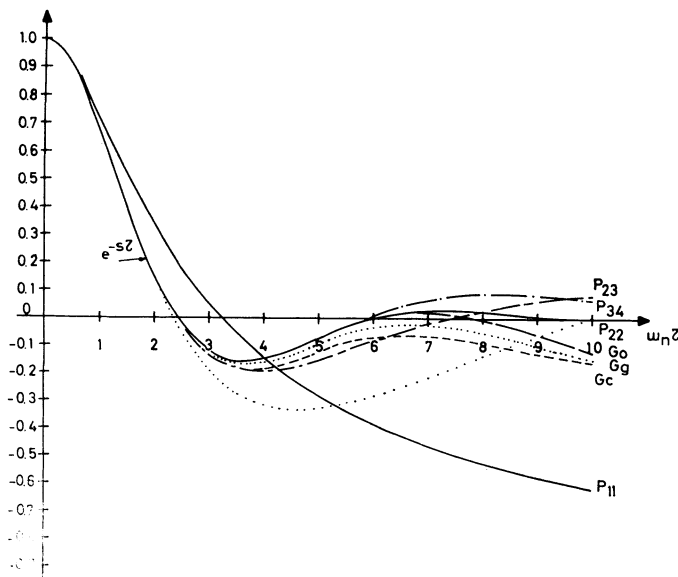
(a)



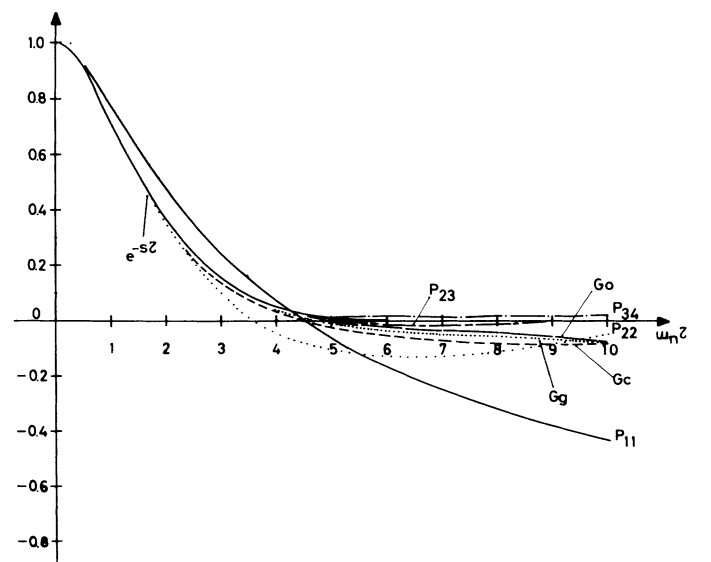
(b)



(d)



(c)



(e)

Fig. 12. Approximate autocorrelation if $H(s)$ is a second-order system for (a) $\xi=0.1$; (b) $\xi=0.2$; (c) $\xi=0.5$; (d) $\xi=0.7$; and (e) $\xi=0.9$.

is given [1] by

$$R_x(\tau) = \frac{A_0^2}{2} \cos \omega_0 \tau, \quad (42)$$

and its power density spectrum is found, according to the Wiener-Khintchine theorem, by

$$W_x(\omega) = 2FR_x(\tau),$$

$$W_x(x) = \frac{A_0^2}{2} \int_{-\infty}^{\infty} [\cos(\omega + \omega_0)\tau + \cos(\omega - \omega_0)\tau] d\tau. \quad (43)$$

But

$$\int_{-\infty}^{\infty} \cos(\omega + \omega_0)\tau d\tau = \lim_{\tau \rightarrow \infty} \frac{\sin(\omega + \omega_0)\tau}{\omega + \omega_0} - \lim_{\tau \rightarrow -\infty} \frac{\sin(\omega + \omega_0)\tau}{\omega + \omega_0}$$

$$= 2 \lim_{\tau \rightarrow \infty} \frac{\sin(\omega + \omega_0)\tau}{\omega + \omega_0} = 2\pi\delta(\omega + \omega_0).$$

In the same way we find

$$\int_{-\infty}^{\infty} \cos(\omega - \omega_0)\tau d\tau = 2\pi\delta(\omega - \omega_0),$$

so that, from (43),

$$W_x(x) = \frac{A_0^2}{2} \cdot 2\pi[\delta(\omega + \omega_0) + \delta(\omega - \omega_0)].$$

The measured value $R_{xa}(\tau)$ may now be found by replacing in (11):

$$R_{xa}(\tau) = \frac{1}{2} \int_{-\infty}^{\infty} G_a(j\omega\tau) W_x(\omega) \frac{d\omega}{2\pi},$$

$$R_{xa}(\tau) = \frac{1}{2} \int_{-\infty}^{\infty} G_a(j\omega\tau) \frac{A_0^2}{2} [\delta(\omega + \omega_0) + \delta(\omega - \omega_0)] d\omega.$$

Because of the property of the delta function we get, finally,

$$R_{xa}(\tau) = \frac{A_0^2}{2} \frac{G_a(j\omega_0\tau) + G_a(-j\omega_0\tau)}{2},$$

or

$$R_{xa}(\tau) = \frac{A_0^2}{2} \operatorname{Re} [G_a(j\omega_0\tau)], \quad (44)$$

where Re stands for "real part of." In fact, if we use a perfect delay,

$$G_a(j\omega_0\tau) = e^{-j\omega_0\tau}, \quad (45)$$

and

$$\operatorname{Re} [G_a(j\omega_0\tau)] = \cos \omega_0 \tau,$$

which, replaced in (44), gives the exact value indicated by (42).

Equation (45) means that, for measuring autocorrela-

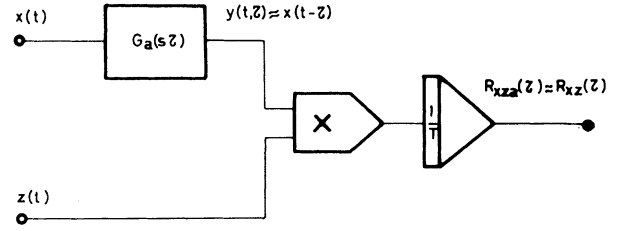


Fig. 13. Circuit for measuring crosscorrelations.

tion of sine waves, the best approximation is one whose response on the $j\omega$ axis (i.e., its frequency response) best approximates the frequency response of the exponential function. This implies a constant amplitude, equal to one, and a linear phase variation with $\omega_0\tau$, since

$$|e^{-j\omega_0\tau}| = 1,$$

and

$$\angle [e^{-j\omega_0\tau}] = -\omega_0\tau.$$

It is in this case that the criterion coincides with that of selecting the delay approximation that has the best frequency response, as described in the literature [2]. For instance, $G_e(j\omega\tau)$ gives a phase error of less than 1.1° from $\omega\tau = 0$ up to $\omega\tau = 7.5$, after which the error increases rapidly. However, $P_{44}(j\omega\tau)$ reaches this same phase error at $\omega\tau = 4.8$, and $P_{34}(j\omega\tau)$ reaches it at $\omega\tau = 4.2$.

EXTENSION TO CROSSCORRELATION MEASUREMENTS

The results obtained for autocorrelation measurements may be extended to include the case of crosscorrelations, the steps to be followed being similar. Let us suppose that it is necessary to measure the crosscorrelation between two signals, $x(t)$ and $z(t)$, using an approximate delay $G_a(s\tau)$ (Fig. 13). The output of $G_a(s\tau)$ will be

$$y(t, \tau) = \int_{-\infty}^{\infty} g_\tau(\tau_1) x(t - \tau_1) d\tau_1, \quad (46)$$

where $g_\tau(\tau_1)$ is the impulse response of $G_a(s\tau)$ for its parameters set at τ .

We may now write the crosscorrelation between $y(t, \tau)$ and $z(t)$, using τ_2 as the corresponding delay, as

$$R_{yz}(\tau_2) = \overline{y(t, \tau) z(t + \tau_2)},$$

and

$$R_{zy}(\tau_2) = R_{yz}(-\tau_2) = \overline{y(t, \tau) z(t - \tau_2)}.$$

If we set $\tau_2 = 0$,

$$R_{zy}(0) = R_{yz}(0) = \overline{y(t, \tau) z(t)},$$

which is what is actually measured by the system of Fig. 13 for each setting of τ . Hence, we may write that the approximate crosscorrelation is

$$R_{xza}(\tau) = R_{yz}(0) = R_{zy}(0).$$

From (46) we have

$$R_{zy}(\tau_2) = R_{yz}(-\tau_2) = \overline{y(t, \tau)z(t - \tau_2)} \\ = \int_{-\infty}^{\infty} g_r(\tau_1) \overline{x(t - \tau_1)z(t - \tau_2)} d\tau_1. \quad (47)$$

Now the crosscorrelation between $x(t - \tau_1)$ and $z(t)$, using τ_2 as the delay parameter, may be written as

$$\overline{x(t - \tau_1)z(t - \tau_2)} = \overline{x(t)z(t - \tau_2 + \tau_1)} = R_{zx}(\tau_1 - \tau_2).$$

But since

$$R_{zx}(\tau_1 - \tau_2) = R_{zx}(\tau_2 - \tau_1), \quad (48)$$

from (47) and (48) we obtain

$$R_{zy}(\tau_2) = R_{yz}(-\tau_2) = \int_{-\infty}^{\infty} g_r(\tau_1) R_{zx}(\tau_2 - \tau_1) d\tau_1.$$

This means $R_{yz}(\tau_2)$ is the convolution between g_r and R_{zx} ; hence its Fourier transform is given [1] by

$$F[R_{zy}(\tau_2)] = \frac{1}{2} W_{zy}(\omega) = \frac{1}{2} G_a(j\omega\tau) W_{zx}(\omega), \quad (49)$$

because $g_r(\tau_1)$ is the impulse response of $G_a(s\tau)$, and also

$$F[R_{zx}(\tau_1)] = \frac{1}{2} W_{zx}(\omega).$$

According to the Wiener-Khinchine theorem we may write that

$$R_{zy}(\tau_2) = \frac{1}{2} \int_{-\infty}^{\infty} e^{j\omega\tau_2} W_{zy}(\omega) \frac{d\omega}{2\pi}, \\ R_{zy}(0) = \frac{1}{2} \int_{-\infty}^{\infty} W_{zy}(\omega) \frac{d\omega}{2\pi}.$$

Replacing (49), we now get

$$R_{zy}(0) = R_{yz}(0) = \frac{1}{2} \int_{-\infty}^{\infty} G_a(j\omega\tau) W_{zx}(\omega) \frac{d\omega}{2\pi}. \quad (50)$$

But we have seen that the measurement is given by $R_{zya}(\tau) = R_{yz}(0)$. Then, according to (50),

$$R_{zya}(\tau) = \frac{1}{2} \int_{-\infty}^{\infty} G_a(j\omega\tau) W_{zx}(\omega) \frac{d\omega}{2\pi}. \quad (51)$$

We observe that (51) is the most general case of (11). Indeed, we need only place $z = x$ in (51) to obtain (11). The conclusions derived for the autocorrelation case may be now extended to crosscorrelation measurements.

CONCLUSIONS

A general equation (11) has been derived which allows the calculation of the correlation function that would be measured if a certain delay approximation were used.

If the noise has a rational spectrum, i.e., if it is generated by passing white noise through a linear lumped parameter filter $H(s)$, (11) turns into (16), subject to certain restrictions. In this case we have found that the best delay approximation depends on the nature of the poles of $H(s)$. In the case of the real simple poles of $H(s)$

the answer is straightforward since, no matter how many poles there may be, the best delay is one whose value for a real argument best approximates the exponential function for a real argument, within the range of delays considered. Low-pass approximations are then to be preferred.

If $H(s)$ is a second-order system, then the selection depends on ξ , the damping factor of the poles. For example, we find that in the case of fourth-order approximations, as ξ decreases, the best delays change from $P_{34}(s\tau)$ for the higher values, to $G_0(s\tau)$ and $G_\theta(s\tau)$ for the lower values.

For complicated rational spectra, in which $H(s)$ may have real and complex poles, the selection of $G_a(s\tau)$ is not so simple. However, we might expect that if, for instance, there are real poles, and complex poles with high damping factors, a low-pass approximation might be better. If there are only complex poles of low ξ , $G_a(s\tau)$ or $G_\theta(s\tau)$ might be preferred.

If the pole pattern of $H(s)$ is arbitrary, for each pole-zero configuration we may find the best approximation $G_a(s\tau)$. In fact, we may calculate the coefficients of $G_a(s\tau)$ by requiring that the mean square of the difference (25) between the actual value of the correlation $R(\tau)$ and the measured value shall be a minimum. This, of course, implies a certain knowledge of the form of $H(s)$ and of the range of variation of its parameters, which in turn determine the pole-zero configuration. Such knowledge exists in the identification problem of adaptive control systems, for instance.

The results contained in this paper may also be used in the case where simultaneous measurement of the correlation values for several values of τ is required. Various delay lines of decreasing complexity may be used, starting with elaborate approximations for high values of τ and using more and more simple delay lines as τ decreases. In this manner, considerable savings in equipment may be effected.

APPENDIX

Following the lines for a similar case [8], we find a sufficient condition so that

$$\lim_{R \rightarrow \infty} \oint_{C_2} f(s) ds = 0 \quad (52)$$

for $s = Re^{j\phi}$. [See (15) and Fig. 4.] Replacing $s = Re^{j\phi}$ in (52) we may write

$$\lim_{s \rightarrow \infty} \oint_{C_2} f(s) ds = \lim_{R \rightarrow \infty} \int_{-\pi/2}^{\pi/2} f(Re^{j\phi}) j Re^{j\phi} d\phi. \quad (53)$$

Also,

$$\left| \int_{-\pi/2}^{\pi/2} f(Re^{j\phi}) j Re^{j\phi} d\phi \right| \leq \int_{-\pi/2}^{\pi/2} |sf(s)| d\phi \quad (54)$$

for $Re^{j\phi} = s$. We see, then, that if

$$\lim_{s \rightarrow \infty} |sf(s)| = 0,$$

integral (53) will also go to zero.

Now, in order that

$$\lim_{s \rightarrow \infty} |sf(s)| = 0,$$

we must have, from (13a),

$$\lim_{s \rightarrow \infty} |sf(s)| = \lim_{s \rightarrow \infty} \left| sG_a(s\tau)W_x\left(\frac{s}{j}\right) \right| = 0. \quad (55)$$

In particular, if $W_x(\omega)$ is the power density spectrum of white noise filtered by a linear lumped parameter system with transfer function $H(j\omega)$, from (17) we have,

$$W_x(\omega) = H(j\omega)H(-j\omega)W_0, \\ W_x\left(\frac{s}{j}\right) = H(s)H(-s)W_0. \quad (56)$$

Then, replacing (56) in (55), the following condition must be fulfilled:

$$\lim_{s \rightarrow \infty} |sG_a(s\tau)H(s)H(-s)| = 0. \quad (57)$$

Since $sG_a(s\tau)H(s)H(-s)$ is a rational fraction, and if the degree of its denominator is greater by more than one with respect to the degree of its numerator, the expression in (57) will have a zero at infinity, (52) will apply, and (16) will be true.

For example, let $G_a(s\tau)$ be of the all-pass type, and let

$$H(s) = K \frac{\sum_{i=0}^m a_i s^i}{\sum_{j=0}^n a_j s^j}.$$

Then, for $sG_a(s\tau)H(s)H(-s)$, we have

$$\begin{aligned} \text{Degree of numerator} &= 1 + \text{degree of } G_a + 2m \\ \text{Degree of denominator} &= 1 + \text{degree of } G_a + 2n. \end{aligned}$$

But condition (57) means that

$$1 + \text{degree of } G_a + 2m + 1 < 1 + \text{degree of } G_a + 2n,$$

so that $2m + 1 < 2n$.

Since m and n are integers, it is sufficient that $m < n$.

REFERENCES

- [1] D. Middleton, *An Introduction to Statistical Communication Theory*, New York: McGraw-Hill, 1960, sect. 1.6, ch. 3 and 16.
- [2] C. H. Single, *Review of Transport Delay Representations for an Analog Computer*, Ann Arbor, Mich.: Applied Dynamics, Inc., 1963.
- [3] H. D. Huskey and G. A. Korn, *Computer Handbook*, New York: McGraw-Hill, 1962, sect 6.1.3.
- [4] W. J. King and V. C. Rideout, *Improved Transport Delay Circuits for Analog Computer Use*, Tucson, Ariz.: U. of Arizona, Electrical Engineering Dept., 1961.
- [5] W. Kaplan, *Operational Methods for Linear Systems*, Reading, Mass.: Addison-Wesley, 1962, sect 3.13.
- [6] W. B. Davenport and W. L. Root, *An Introduction to the Theory of Random Signals and Noise*, New York: McGraw-Hill, 1958, sect. 9.3.
- [7] J. G. Truxal, *Automatic Feedback Control System Synthesis*, New York: McGraw-Hill, 1955, sect. 9.8.
- [8] W. Kaplan, *Advanced Calculus*, Reading, Mass.: Addison-Wesley, 1957, p. 577.

Experimental Study of a New Method of Time Delay for Analog Computers

WALTER W. WIERWILLE, MEMBER, IEEE

Abstract—A new method for obtaining pure delay of voltage waveforms on the analog computer is discussed. This method, which is based upon frequency-domain sampling in combination with a feedforward-feedback technique, is capable of producing relatively long delays. The theory underlying the method has been previously presented. In this paper experimental aspects are described in detail. Particular emphasis is placed upon those topics that are important to the use of the method in actual practice, namely; 1) a general, scaled computer diagram, 2) typical experimental records (which also verify the theory), and 3) a general procedure for programming and de-

bugging. The experimental study has shown that high-quality results are obtainable with this method. Moreover, it is widely applicable to computation and simulation problems, and can easily be programmed.

INTRODUCTION

A NEW METHOD for obtaining continuous delay of signals on the analog computer was recently evolved [1]. This new delay technique makes use of feedforward and feedback loops in conjunction with a series of frequency-domain sampling filters [2], [3]. Only standard linear analog computing components are required. Although the theory of the new method of

Manuscript received September 21, 1964.

The author is with the Cornell Aeronautical Laboratory, Inc., of Cornell University, Buffalo, N. Y.